Chapter 4

Magnetic anisotropy, magnetic domains and superparamagnetism

Suggested Reading
For background:
Chapter 3 (pp. 41-55) Butler (1992)
General background in Statistical Mechanics (see, e.g.,
http://en.wikipedia.org/wiki/Statistical_mechanics)
To learn more:
Chapter 2.8 & 5 Dunlop and Özdemir (1997)

4.1 Introduction

In Lecture 3 we learned that in some crystals electronic spins work in concert to create a spontaneous magnetization that remains in the absence of an external field. The basis of paleomagnetism is that these ferromagnetic particles carry the record of ancient magnetic fields. What allows the magnetic moments to come into equilibrium with the geomagnetic field and then what fixes that equilibrium magnetization into the rock so that we may measure it millions or even billions of years later? We will begin to answer these questions over the next few lectures.

We will start with the second part of the question: what fixes magnetizations in particular directions? The short answer is that certain directions within magnetic crystals are at lower energy than others. To shift the magnetization from one "easy" direction to another requires energy. If the barrier is high enough, the particle will stay magnetized in the same direction for very long periods of time - say billions of years. In this lecture we will address what causes and some of the consequences of these energy barriers.

4.2 The magnetic energy of particles

4.2.1 Magnetic moments and external fields

We know from experience that there are energies associated with magnetic fields. Just as a mass has a potential energy when it is placed in the gravitational field of another mass, a magnetic moment has an energy when it is placed in a magnetic field. We have seen this energy briefly in

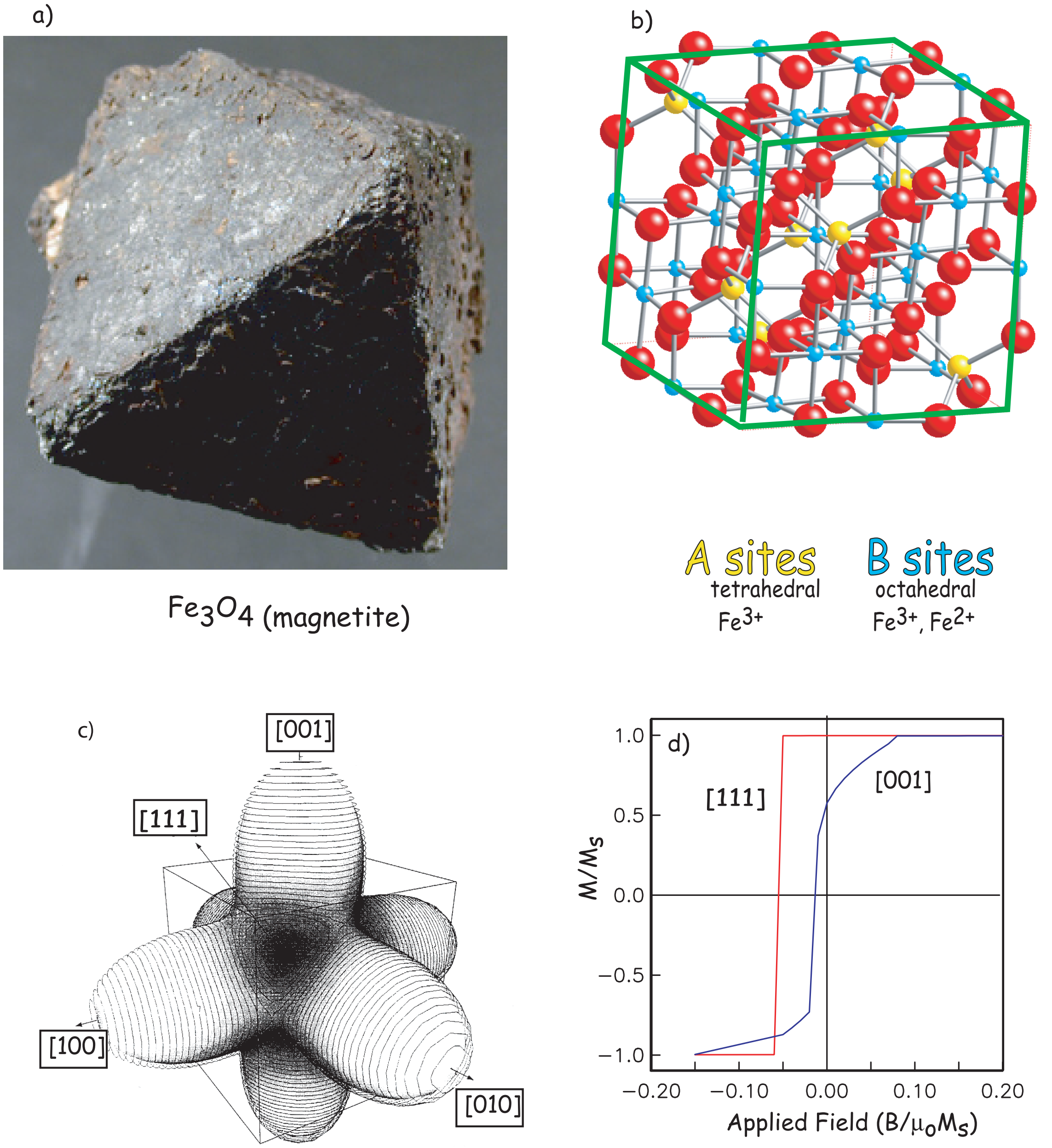

Figure 4.1: a) A magnetite octahedron. b) Internal crystal structure. Big red dots are the oxygen anions. The blue dots are iron cations in octahedral coordination and the yellow dots are in tetrahedral coordination. Fe^{3+} sits on the A sites and Fe^{2+} and Fe^{3+} sit on the B sites. c) Magnetocrystalline anisotropy energy as a function of direction within a magnetite crystal. The easiest direction to magnetize (the direction with the lowest energy) is along the body diagonal. (Redrawn from Williams and Dunlop, 1995.) d) Numerical simulation of the magnetization of a cube of magnetite as the applied field is brought down from saturation to zero, then changed sign and increased again in the opposite direction along two directions in the crystal. The magnetization when aligned with the body diagonal [111] direction (which is associated with the minimum energy state - see c) - is harder to change than along one of the "hard" directions (e.g. [001]).

Lectures 1 and Lecture 3 as the magnetostratic energy ($\mathbf{m} \cdot \mathbf{B}$). This energy has many names, but here we will work with the volume normalized "magnetostatic interaction energy density" (E_b):

$$E_b = -\mathbf{M} \cdot \mathbf{B}. \tag{4.1}$$

E_b is at a minimum when the magnetization $\mathbf{M}$ is aligned with the field $\mathbf{B}$. It is this energy that drives magnetic compass needles to seek the minimum energy state by aligning themselves with the ambient magnetic field.

4.2.2 Exchange energy

We learned in Lecture 3 that some crystalline states are capable of ferromagnetic behavior because of quantum mechanical considerations. Electrons in neighboring orbitals in certain crystals "know" about each other's spin states. In order to avoid sharing the same orbital with the same spin (hence having the same quantum numbers - not allowed from Pauli's exclusion principle), electronic spins in such crystals act in a coordinated fashion. They will be either aligned parallel or antiparallel according to the details of the interaction. This *exchange energy density* (E_e) is the source of spontaneous magnetization and is given for a pair of spins by:

$$E_e = -2J_e \mathbf{S}_i \cdot \mathbf{S}_j$$

where J_e is the "exchange integral" and $\mathbf{S}_i$ and $\mathbf{S}_j$ are spin vectors. Depending on the details of the crystal structure (which determines the size and sign of the exchange integral), exchange energy is at a minimum when electronic spins are aligned parallel or anti-parallel.

We define here a parameter that we will use later: the exchange constant $A = J_e S^2/a$ where a is the interatomic spacing. $A = 1.33 \text{ x } 10^{-11}$ Jm^{-1} for magnetite, a common magnetic mineral.

The $3d$ electronic orbitals within magnetic crystals are, unlike the s orbitals, anisotropic (recall Lecture 3). They "poke" in certain directions. Hence spins in some directions within crystals will be easier to coordinate than in others. We can illustrate this using the example of magnetite shown in Figure 4.1. Magnetite octahedra (Figure 4.1a), when viewed at the atomic level (Figure 4.1b) are composed of one ferrous (Fe^{2+}) cation, two ferric (Fe^{3+}) cations and four O^{2-} anions. Each oxygen anion shares an electron with two neighboring cations in a covalent bond.

In Lecture 3 it was mentioned that in some crystals, spins are aligned anti-parallel, yet there is still a net magnetization, a phenomenon known as "ferrimagnetism". This can arise from the fact that not all cations have the same number of unpaired spins. Magnetite, with its ferrous (4 m_b) and ferric (5 m_b) states is a good example. There are three iron cations in a magnetite crystal giving a total of 14 m_b to play with. This is HUGE. Magnetite is very magnetic, but not that magnetic! From Figure 4.1b we see that the ferric ions are all sitting on the tetrahedral (A) lattice sites and there are equal numbers of ferrous and ferric ions sitting on the octahedral (B) lattice sites. The unpaired spins of the cations in the A and B lattice sites are aligned anti-parallel to one another because of super exchange (Lecture 3) so we have 9 m_b on the B sites minus 4 m_b on the A sites for a total of 5 m_b per unit cell of magnetite.

4.2.3 Magnetocrystalline anisotropy energy

The energy of moments aligned along different directions in magnetite is shown in Figure 4.1c. The bulges are in directions that have the highest energy ([001, 010, 100]). The lowest energy is along the body diagonal ([111] direction). The energy surface shown in Figure 4.1c represents the *magnetocrystalline anisotropy energy*, E_a. In a cubic crystal with direction cosines $\alpha_1, \alpha_2, \alpha_3$ (the cosines of the angles between the direction and the crystallographic axes [100, 010, 001]; see appendix to Lecture 1), the energy density is given by:

$$E_a = K_1(\alpha_1^2\alpha_2^2 + \alpha_2^2\alpha_3^2 + \alpha_3^2\alpha_1^2) + K_2\alpha_1^2\alpha_2^2\alpha_3^2 \tag{4.2}$$

where K_1 and K_2 are empirically determined *magnetocrystalline anisotropy constants.* In the case of (room temperature) magnetite, K_1 is -1.35 x 10^4 Jm^{-3}. If you work through the magnetocrystalline equation, you will find E_a is zero parallel to the [100] axis, $K_1/4$ parallel to the [110] and $K_1/3 + K_2/27$ parallel to the [111] direction (the body diagonal). So when K_1 is negative, the [111] direction has the minimum energy. This is the reason that there is a dimple in the energy surface along that direction in Figure 4.1c.

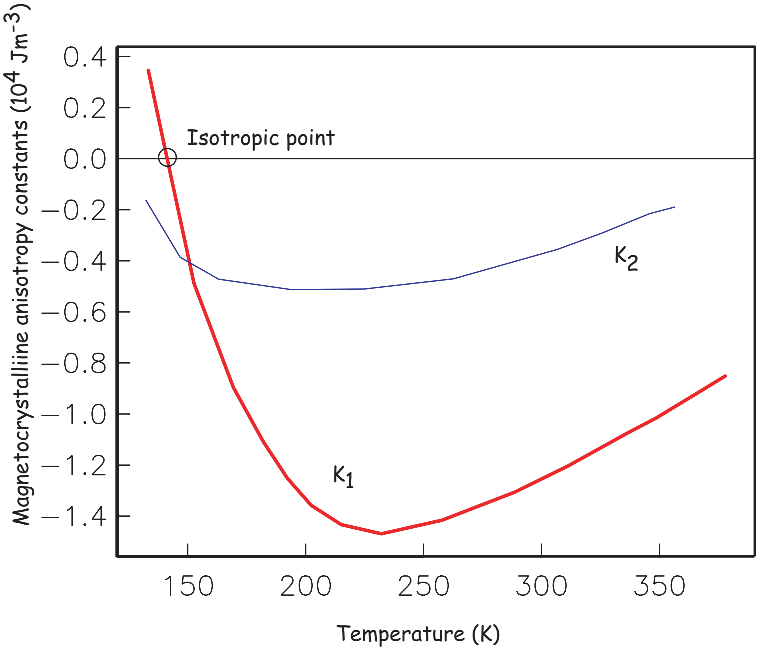

Figure 4.2: Variation of K_1 and K_2 of magnetite as a function of temperature. Redrawn from Dunlop and Özdemir (1997).

As a consequence of the magnetocrystalline anisotropy energy, once the magnetization is aligned with an easy direction, work must be done to change it. In order to switch from one easy axis to another (e.g. from one direction along the body diagonal to the opposite), the magnetization has to traverse a path over an energy barrier which is the difference between the energy in the easy direction and that in the intervening hard direction. In the case of magnetite at room temperature, we have this energy barrier as E[111]-E[110] or to first order $K_1/3 - K_1/4 = K_1/12$.

In Figure 4.1d we show the results of numerical simulations of the magnetization of a cube of magnetite as an applied field is brought from saturation to zero, then changed in sign and increased in the opposite direction. We show the results from two directions in the crystal. The magnetization aligned with the body diagonal [111] (associated with the minimum energy state - see Figure 4.1c) is harder to change than along one of the "hard" directions (e.g. [001]).

A useful parameter in characterizing the stability of a particular particle or assemblage of particles is the field that is required to drive the magnetizations out of the easy directions, over an energy barrier and into another easy direction. This field is called the flipping field, the coercive field or the coercivity (B_c or H_c depending on units), something we will consider in more detail in later lectures.

Cubic symmetry (as in the case of magnetite) is just one of many types of crystal symmetries. One other very important form is the uniaxial symmetry which can arise from crystal shape or structure. The energy density for uniaxial magnetic anisotropy is:

$$E_a = K_{u1} sin^2\theta + K_{u2} \sin^4\theta + ... \tag{4.3}$$

In this equation, when the "uniaxial anisotropy constant", K_u, is negative, the magnetization is constrained to lie perpendicular to the axis of symmetry. When $K_u > 0$, the magnetization lies parallel to it.

An example of a mineral dominated by uniaxial symmetry is hematite. The magnetization of hematite is quite complicated, as we shall learn later, but one source is magnetization lies in the "spin-canting" (see Lecture 3) within the basal plane of a hexagonal crystal. Within the basal plane, the anisotropy constant is very low and the magnetization wanders fairly freely. However, the anisotropy energy away from the basal plane is high, so the magnetization is constrained to lie within the basal plane.

Because electronic interactions depend heavily on inter atomic spacing, magnetocrystalline anisotropy constants are a strong function of temperature (see Figure 4.2). In magnetite, K_1 changes sign at a temperature known as the "isotropic point". At the isotropic point, there is no large magnetocrystalline anisotropy. The large energy barriers that act to keep the magnetizations parallel to the body diagonal are gone and the spins can wander more freely through the crystal. Below the isotropic point, the energy barriers rise again, but with a different topology in which the crystal axes are the energy minima and the body diagonals are the high energy states.

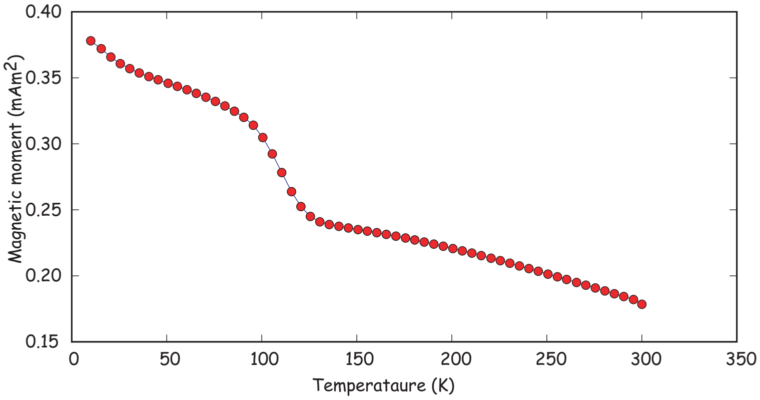

Figure 4.3: Magnetization curve for magnetite as a function of temperature. The specimen was placed in a very large field, cooled to near absolute zero, then warmed up. The magnetization was measured as it warmed. goes through the Verwey transition, a fraction of the magnetization is lost. Data downloaded from "w5000" in the "Rock magnetic Bestiary" collection at the Institute for Rock Magnetism (http://www.irm.umn.edu/bestiary/).

At room temperature, electrons hop freely between the ferrous and ferric ions on the B lattice sites, so there is no order. Below about 120 K, there is an ordered arrangement of the ferrous and ferric ions. Because of the difference in size between the two, the lattice of the unit cell becomes slightly distorted and becomes monoclinic instead of cubic. This transition is known as the *Verwey transition.* Although the isotropic point (measured magnetically) and the Verwey transition (measured electrically) are separated in temperature by about 15^o, they are related phenomena (the ordering and electron hopping cause the change in K_1).

The change in magnetocrystalline anisotropy at low temperature can have a profound effect on the magnetization. In Figure 4.3 we show a typical (de)magnetization curve for magnetite taken from the "Rock magnetic bestiary" web site maintained at the Institute for Rock Magnetism: http://www.geo.umn.edu/orgs/irm/bestiary. There is a loss of magnetization at around 100 K. This loss is the basis for "low-temperature demagnetization" (LTD). However, some portion of the magnetization is always recovered after low temperature cycling (called the *low temperature memory*), so the general utility of LTD is somewhat limited.

4.2.4 Magnetostriction - stress anisotropy

Because the exchange energy depends strongly on the details of the physical interaction between orbitals in neighboring atoms with respect to one another, changing the positions of these atoms will affect that interaction. Put another way, straining a crystal will alter its magnetic behavior. Similarly, changes in the magnetization can change the shape of the crystal by altering the shapes of the orbitals. This is the phenomenon of *magnetostriction.* The magnetic energy caused by the application of stress to a crystal be approximated by:

$$E_\sigma = -\frac{3}{2}\bar{\lambda}\sigma \sin^2\theta$$

where $\bar{\lambda}$ is an experimentally derived constant, σ is the stress, and θ is the angle of the stress with with respect to the c crystallographic axis. $\bar{\lambda}$ for magnetite is about 40 x 10^{-6}. Note the similarity in form of magnetostriction and uniaxial anisotropy giving rise to a single "easy axis" within the crystal.

4.2.5 Magnetostatic - or shape anisotropy

There is one more important source of magnetic anisotropy: shape. To understand how crystal shape controls magnetic energy, we need to understand the concept of the internal "demagnetizing field" of a magnetized body. In Figure 4.4a we show the magnetic vectors within a ferromagnetic crystal. These produce a magnetic field external to the crystal that is proportional to the magnetic moment (see Lecture 1). This external field is identical to a field produced by a set of "free poles" distributed over the surface of the crystal (Figure 4.4b). The surface poles don't just produce the external field, they also produce an internal field shown in Figure 4.4c. The internal field is known as the *demagnetizing field* H_d. H_d is proportional to the magnetization of the body and is sensitive to the shape. For the simple ellipsoid shown in Figure 4.4, the demagnetizing field is given by:

$$\mathbf{H}_d = -N\mathbf{M}$$

where N is a *demagnetizing factor* determined by the shape. For a sphere, the surface poles are distributed over the surface such that there are none at the "equator" and most at the "pole" (see Figure 4.4d). By using tricks of potential field theory in which we can pretend that the external

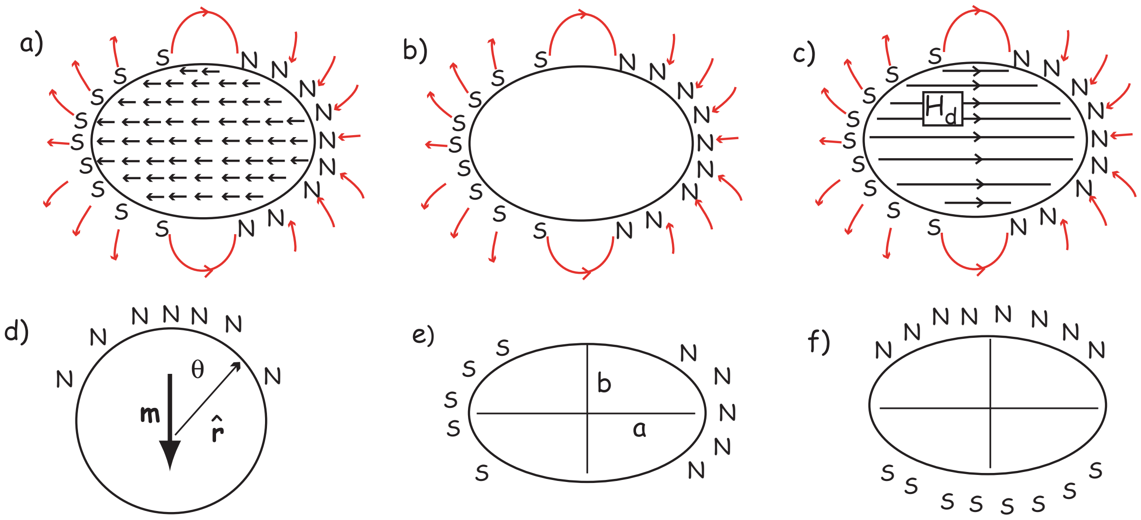

Figure 4.4: a) Internal magnetizations within a ferromagnetic crystal. b) Generation of an identical external field from a series of surface monopoles. c) The internal "demagnetizing" field resulting from the surface poles. [Redrawn from O'Reilly, 1984]. d) Surface poles on a sphere. e) Surface poles on an ellipse, with the magnetization parallel to the elongation. f) Surface poles with the magnetization perpendicular to the axis of elongation.

field of a uniformly magnetized body is identical to that of a central dipole moment of magnitude $m = vM$ (where v is volume). At the equator of the sphere as elsewhere, $\mathbf{H}_d = -N\mathbf{M}$. But the external field at the equator equal to the demagnetizing field just inside the body because the field is continuous across the body. The equatorial (tangential) field at the equator (remembering from Lecture 1) is given by

$$H_e = -\frac{m}{4\pi r^3}.$$

Using the fact that that magnetization (in units of Am^{-1}) is the moment (in units of Am^2) per unit volume (in units of m^3) and the volume of a sphere is $\frac{4}{3}\pi r^3$, we have:

$$m = \frac{4}{3}\pi r^3 M,$$

so substituting and solving for H_d we get $H_d = -\frac{1}{3}M$, hence $N = \frac{1}{3}$.

Different directions within a non-spherical crystal will have different distributions of free poles (see Figures 4.4e,f). In fact the surface density of free poles is given by $\sigma_m = \mathbf{M} \cdot \hat{r}$. Because the surface pole density depends on direction, so too will N. In the case of an ellipsoid magnetized parallel to the elongation axis a (Figure 4.4e), the free poles are farther apart than across the grain, hence, intuitively, the demagnetizing field, which depends on $1/r^2$, must be less than in the case of a sphere. Thus, $N_a <\frac{1}{3}$. Similarly, if the ellipsoid is magnetized along b (Figure 4.4e), the demagnetizing field is stronger or $N_b > \frac{1}{3}$. In an ellipsoid there are three axes a, b, c, and $N_a + N_b + N_c = 1$ (in SI; in cgs units the sum is 4π). This plus the fact that $N_a = \frac{1}{3}[1 - \frac{2}{5}(2 - \frac{b}{a} - \frac{c}{a})]$ allows us to determine $N_{a,b,c}$ for any ellipsoid.

Getting back to the anisotropy energy, that arising from the external field of the particle is called *magnetostatic self energy* (sometimes called "self energy") whose energy density equation is:

$$E_{ms} = \frac{1}{2}\mu_o N_a M^2 + \frac{1}{2}\mu_o (N_c - N_a) M^2 \sin^2\theta \tag{4.4}$$

where N_c and N_a are the demagnetizing coefficients along the short and long axes respectively. This expression can be derived by "building" a magnetic particle and considering the potential energy gained by each volume dv as it is brought in $(-\mu_o \mathbf{M} dv \cdot \mathbf{H}_d)$ and integrating. The $\frac{1}{2}$ appears in order to avoid counting each volume element twice and the v dissappears because all the energies we have been discussing are energy densities - the energy per unit volume. Note that the magnetostatic energy has a uniaxial form with the constant of uniaxial anisotropy - $K_u = \frac{1}{2}\Delta N \mu_o M^2$.

For a prolate ellipsoid $N_c = N_b$ and $a/c = 1.5$, $N_a - N_c = \sim 0.16$. The magnetization of magnetite is 4.8 x 10^5Am^{-1}, so $K_u \simeq$ 2.7 x 10^4 Jm^{-3}. This is somewhat larger than the absolute value of K_1 for magnetocrystalline anisotropy in magnetite (K_1= -1.35 x 10^4 Jm^{-3}), so the magnetization for even slightly elongate grains will be dominated by uniaxial anistropy controlled by shape. Minerals with low saturation magnetizations (like hematite) will not be prone to shape dominated magnetic anisotropy, however.

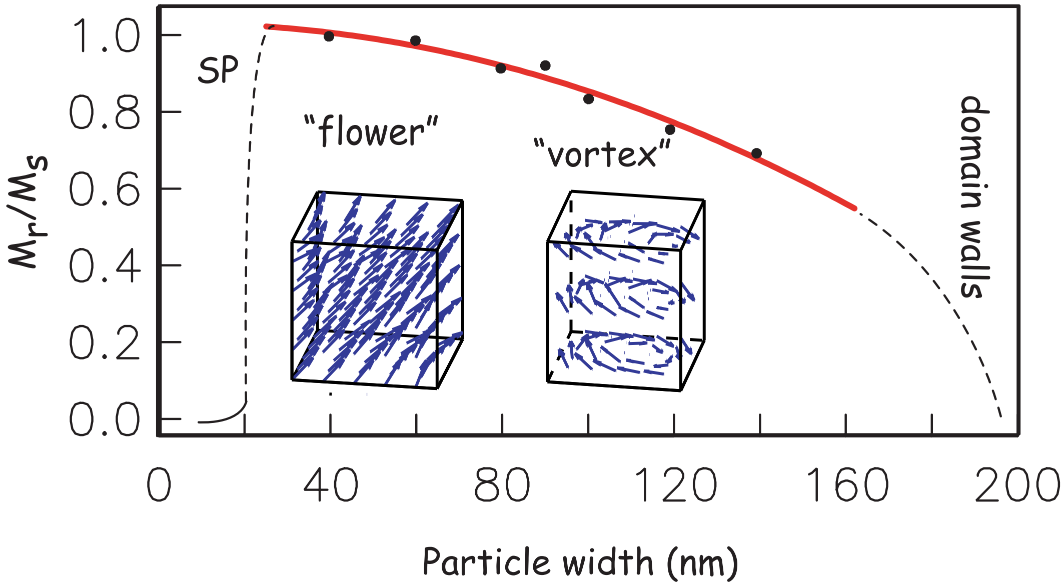

Figure 4.5: Possible non-uniform magnetization configurations that reduce self energy for magnetite with increasing particle widths. The net remanent magnetization reduces with increasingly non-uniform spin configurations. [Data from Tauxe et al., 2002.]

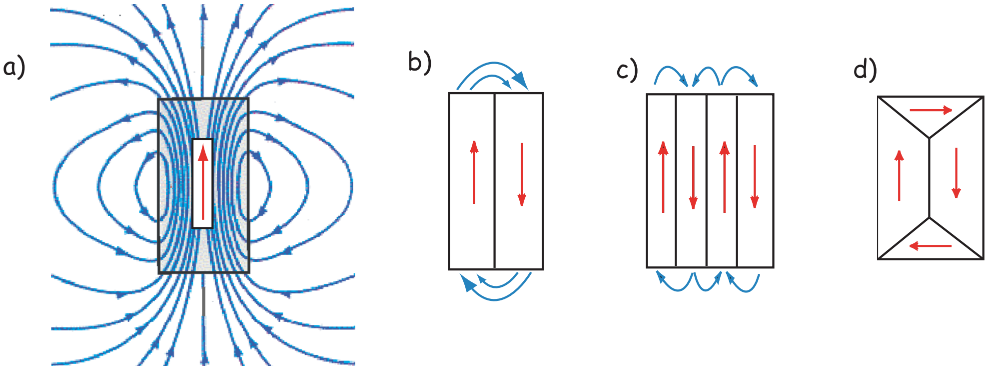

Figure 4.6: A variety of domain structures of a given particle. a) Uniformly magnetized (single domain). b) Two domains. c) Four domains in a lamellar pattern. d) Essentially two domains with two closure domains.

4.3 Magnetic domains

4.3.1 Some theory

So far we have been discussing hypothetical magnetic particles that are uniformly magnetized. In Figure 4.4a we noted that there is an energy associated with the field generated by a magnetic particle. This *self energy* density is given in the simple case when H_d is antiparallel to the internal magnetization by:

$$E_{self} = -\frac{1}{2}\mu_o \mathbf{M} \cdot \mathbf{H}_d = \frac{1}{2}\mu_o N M^2 \tag{4.5}$$

Particles with strong magnetizations (like magnetite) have self energies that quickly become quite large. We have been learning about several mechanisms that tend to align magnetic spins. In fact in very small particles, the spins are essentially lined up. The particle is uniformly magnetized and is called *single domain* (SD). In larger particles (although still pretty small) the self energy exceeds the other exchange and magnetocrystalline energies and crystals have non-uniform states of magnetization.

There are many strategies possible for magnetic particles to reduce self energy. Numerical models (called micromagnetic models) can find internal magnetization configurations that minimize the energies discussed in the preceding sections. Micromagnetic simulations for magnetite particles (e.g. Schabes and Bertram, 1988) allow us to peer into the state of magnetization inside magnetic particles. These simulations give a picture of increasing complexity from so-called “flower” to “vortex” states (Figure 4.5) remanent states.

As particles grow even larger, they break into regions of uniform magnetization called *magnetic domains* separated by narrow zones of rapidly changing spin directions called *domain walls*. Magnetic domains can take many forms. We illustrate a few in Figure 4.6. The uniform case (single domain) is shown in Figure 4.6a. The external field is very large because the free poles are far apart (at opposite ends of the particle). When the particle organizes itself into two domains (Figure 4.6b), the external field is reduced by about a factor of two. In the case of four lamellar domains (Figure 4.6c), the external field is quite small. The introduction of *closure domains* as in Figure 4.6d reduces the external field to nothing.

As you might already suspect, domain walls are not "free". If, as in Figure 4.7a, the spins simply switch from one orientation to the other abruptly, the exchange energy cost would be very high. One way to get around this to spread the change over several hundred atoms, as sketched in Figure 4.7b. The wall width δ is wider and the exchange energy price is much less. However, there are now spins in unfavorable directions from a magnetocrystalline point of view (they are in "hard" direction). Exchange energy therefore favors wider domain walls while magnetocrystalline anisotropy favors thin walls. With some work (see e.g., Dunlop and Özdemir, 1997, pp. 117-118), it is possible to come up with the following analytical expressions for wall width (δ_w) and wall energy density ($\mathbf{E}_w$):

$$\delta_w = \pi(\frac{A}{K})^{\frac{1}{2}}, E_w = 2\pi(AK)^{\frac{1}{2}} \tag{4.6}$$

where A is the exchange constant from before and K is the magnetic anisotropy constant (e.g., K_u or K_1). Plugging in values for magnetite given previously we get δ_w = 0.28 μm and E_w = 2.3 x 10^{-3}Jm^{-2}.

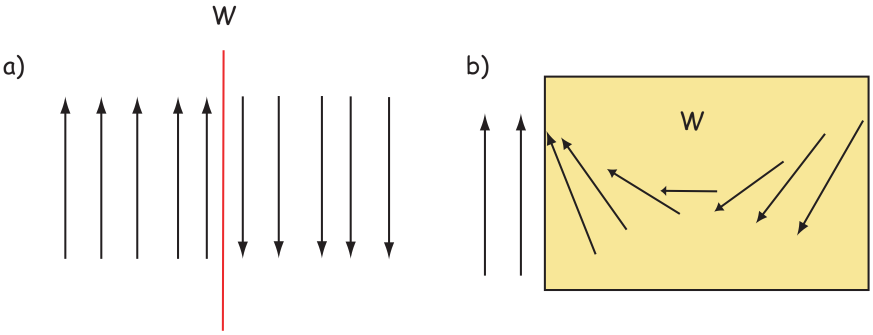

Figure 4.7: Examples of possible domain walls. a) There is a 180° switch from one atom to the next. The domain wall is very thin, but the exchange price is very high. b) There is a more gradual switch from one direction to the other [note: each arrow represents several 10's of unit cells]. The exchange energy price is lower, but there are more spins in unfavorable directions from a magnetocrystalline point of view.

In Figure 4.8 we plot the self energy and the wall energy from E_w for spheres of magnetite. We see that the wall energy in particles with radii of a few tenths of a micron is much less than the self energy, yet the width of the walls is also a few tenths of a micron. So the smallest wall is really more like the vortex state and it is only for particles closer to one micron in size that true domains separated by discrete walls are formed.

It is possible to predict the number of domains (n_d) in a given particle of magnetite. Assuming lamellar domains within cubes of magnetite, Dunlop and Özdemir (1997) derived the following equation:

$$n_d = Z \cdot \frac{b}{a} a^{\frac{1}{2}} \tag{4.7}$$

where Z is a constant incorporating magnetostriction and wall energy and a and b are particle length and width as before. For magnetite, $Z \simeq$1.1 x 10^3. We would expect to find 11 domains in a 100 μm equant grain of magnetite, for example.

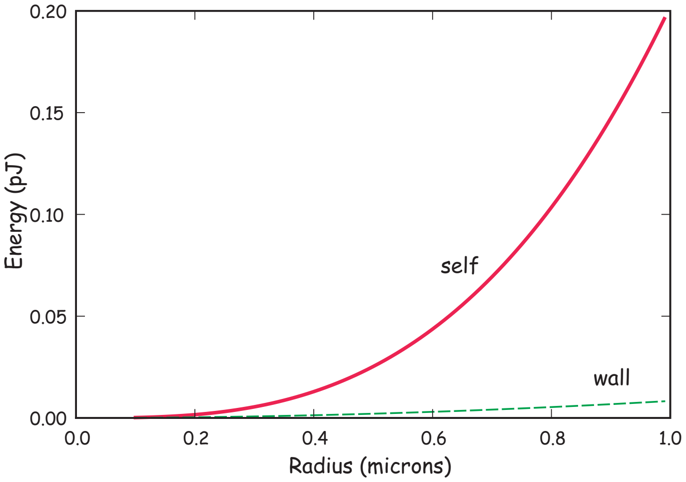

Figure 4.8: Comparison of "self" energy versus the energy of the domain wall in magnetite spheres as a function of particle size.

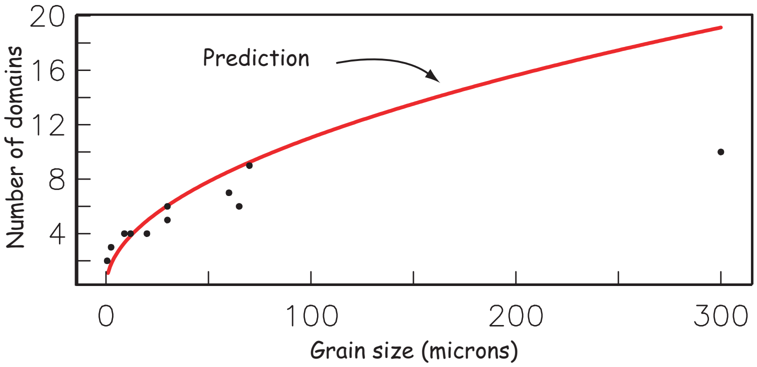

Figure 4.9: Number of domains in magnetite particles versus grain size. Solid curve: predicted values from theory (see text). Dots: data compiled by Özdemir and Dunlop (1997).

4.3.2 Some experiments

How can we test the theoretical predictions of domain theory? Do domains really exist? Are they the size and shape we expect? Are there as many as we would expect? In order to address these questions we require a way of "seeing" magnetic domains. Bitter (1931) devised a way for doing just that. Magnetic domain walls are regions with large stray fields (as opposed to domains in which the spins are usually parallel to the sides of the crystals to minimize stray fields). In the "Bitter technique" magnetic colloid material is drawn to the regions of high field gradients on highly polished sections allowing the domain walls to be observed.

We show an example of a photomicrograph taken from the interior of a large grain of magnetite (Dunlop and Özdemir, 1997) in Figure 4.10. It appears that if great care is taken, domain walls of about the right size, shape and orientation can be found.

Özdemir and Dunlop (1997) compiled what they considered to be the "best" data on number of domains n_d observed in carefully sized magnetite grains. We replot their data compilation in Figure 4.9. Also shown is the prediction from Equation 4.7. There appear to be "too many" domains for small grain sizes and "too few" for large grain sizes. In a seminal paper, Halgedahl and Fuller (1980) argued that there were far fewer domains than predicted for titanomagnetite, which they explained as arising from the fact that the energy to nucleate a domain wall from nothing had not been taken into account in the theory.

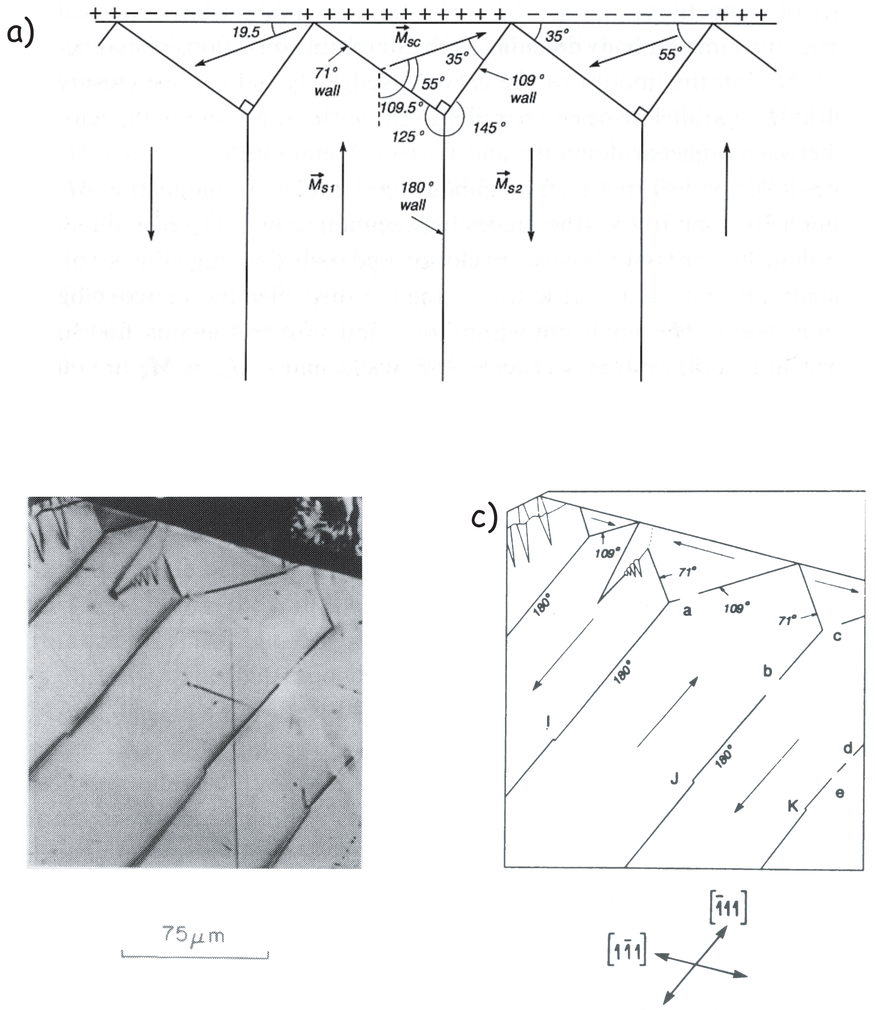

Figure 4.10: a) Theoretical predictions of possible domain structures for magnetite. b) Bitter patterns from an oriented polished section of magnetite. c) Interpretation of the magnetization. [Figures from Dunlop and Ozdemir (1997)].

4.4 Thermal energy

We have gone some way to answering the questions posed at the beginning of the lecture. We see now that it is the anisotropy energy which opposes changes in the magnetic direction, that preseres the magnetization for posterity. We also asked the question of what allows the magnetization to come into equilibrium with the applied magnetic field in the first place; this question requires a little more work to answer. The key to this question is to find some mechanism which allows the moments to “jump over” magnetic anisotropy energy barriers. One such mechanism is thermal energy E_T, which is given by:

$$E_T = kT$$

where kT is thermal energy (see Lecture 3).

We know from statistical mechanics that the probability of finding a grain with a given thermal energy is $P = \exp(-E_T/kT)$. So we may have to wait some time t for a particle to work itself up to having sufficient energy to flip over the energy barrier.

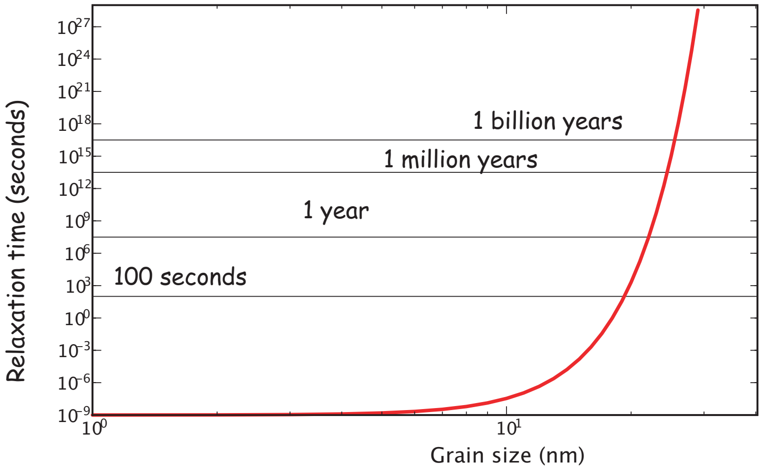

Figure 4.11: Relaxation time as a function of grain size in nanometers.

Imagine a block of material containing a random assemblage of magnetic particles that are for simplicity uniformly magnetized and dominated by uniaxial anisotropy. Suppose that this block has some initial magnetization M_o and is placed in an environment with no ambient magnetic field. Anisotropy energy will tend to keep each tiny magnetic moment in its original direction and the magnetization will not change over time. At some temperature, certain grains will have sufficient energy to overcome the anisotropy energy and flip their moments to the other easy axis. As the energy surface is spherical, with no dimples or protruberances, there is no preferred direction and, over time, the magnetic moments will become random. Therefore, the magnetization as a function of time in this simple scenario will decay to zero. The equation governing this decay is:

$$M(t) = M_o \exp\left(\frac{-t}{\tau}\right) \tag{4.8}$$

where t is time and τ is an empirical constant called the *relaxation time*. Relaxation time is the time required for the remanence to decay to $1/e$ of M_o. This equation is the essence of what is called “Néel theory” (see, e.g., Néel, 1955).

The value of τ depends on the competition between magnetic anisotropy energy and thermal energy. It is a measure of the probability that a grain will have sufficient thermal energy to overcome the anisotropy energy and switch its moment. Therefore in zero external field:

$$\tau = \frac{1}{C} \exp \frac{[\text{anisotropy} \quad \text{energy}]}{[\text{thermal} \quad \text{energy}]} = \frac{1}{C} \exp \frac{[Kv]}{[kT]}, \tag{4.9}$$

where C is a frequency factor with a value of something like 10^{10} s^{-1}. The anisotropy energy is given by the dominant anisotropy parameter K (either K_u, K_1, or λ) times the grain volume v. It is often convenient to use the relationship $K = \frac{B_c M_s}{2}$, which will be derived as a homework assignment.

Thus, the relaxation time is proportional to coercivity, and volume, and is inversely related to temperature. Relaxation time τ varies rapidly with small changes in v and T. To see how this works, we can take K_u for slightly elongate cuboids of magnetite ($b/a = 0.8$) and evaluate relaxation time as a function of particle width (see Figure 4.11). There is a sharp transition between grains with virtually no stability (τ) is on the order of seconds) and grains with stabilities of billions of years.

Grains with $\tau \simeq 10^2 - 10^3$ seconds have sufficient thermal energy to overcome the anisotropy energy frequently and are unstable on a laboratory time-scale. In zero field, these grain moments will tend to rapidly become random and in an applied field, they tend to rapidly align with the field. The net magnetization is related to the field by a Langevin function (see Lecture 3). Therefore, this behavior is quite similar to paramagnetism, hence these grains are called *superparamagnetic* (SP). Such grains can be distinguished from paramagnets, however, because the field required to saturate the moments is typically much less than a tesla, whereas that for paramagnets can exceed hundreds of tesla.

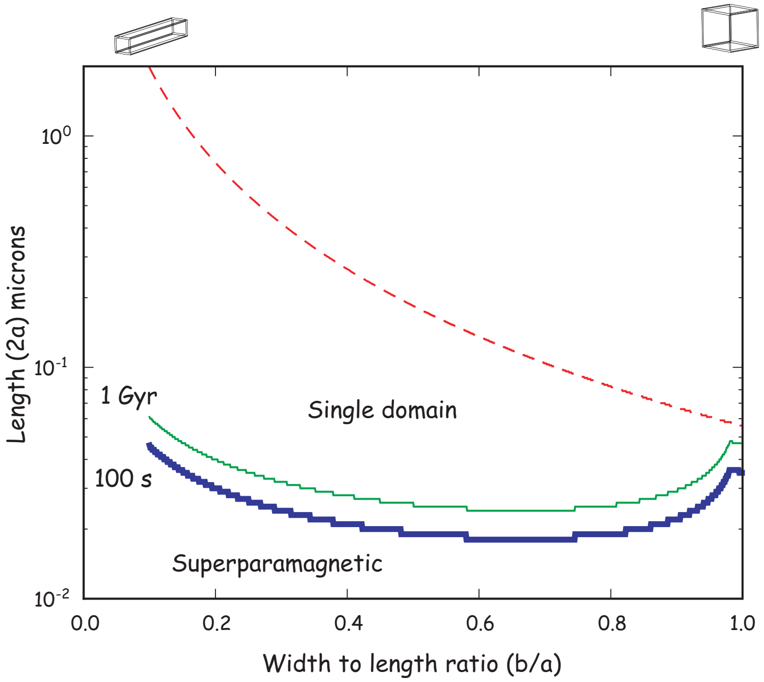

Figure 4.12: Expected domain states for various sizes and shapes of parallelopipeds of magnetite at room temperature. The parameters a and b are as in Figure 4.4. Calculations done using assumptions and parameters described in the text.

4.5 Putting it all together

We are now in a position to pull together all the threads we have considered in this lecture and make a plot of what sort of magnetic particles behave as superparamagnets, which should be single domain and which should be multi-domain according to our simple theories. We can estimate the superparamagnetic to single domain threshold for magnetite as a function of particle shape by finding for the length (2a) that gives a relaxation time of 100 seconds as a function of width to length ratio (b/a) for parallelopipeds of magnetite (heavy blue line in Figure 4.12). To do this, we follow the logic of Butler and Banerjee (1975). In this diagram, we estimated relaxation time using Equation 4.9, plugging in values of K as either the magnetocrystalline effective anisotropy constant ($\frac{1}{12}K_1$) or the shape anisotropy constant ($\frac{1}{2}\Delta N\mu_o M^2$), whichever was less. We also show the curve at which relaxation time is equal to 1 Gyr, reinforcing the point that very small changes in crystal size and shape make profound differences in relaxation time. The figure also predicts the boundary between the single domain field and the two domain field, when the energy of a domain wall is less than the self energy of a particle that is uniformly magnetized. This can be done by evaluating wall energy with Equation 4.6 for a wall along the length of a parallelopiped and area ($4ab$) as compared to the self energy ($\frac{1}{2}\mu_o N_a M^2 v$) for a given length and width to length ratio. When the wall energy is less than the self energy, we are in the two domain field.

Figure 4.12 suggests that there is virtually no SD stability field for equant magnetite; particles are either SP or MD (multi-domain). As the width to length decreases (the particle gets longer), the stability field for SD magnetite expands. Of course micromagnetic modelling shows that there are several transitional states between uniform magnetization (SD) and MD, i.e. the flower and vortex remaent states (see Fabian et al., 1996), but Figure 4.12 has enormous predictive power and the version of Butler and Banerjee (1975), (which is slightly different in detail) continues to be used extensively.